Biomass Conversion and Biorefinery (2023) 13:11187–11201
https://doi.org/10.1007/s13399-021-02183-5

ORIGINAL ARTICLE

Investigation of thermal degradation kinetics and catalytic pyrolysis of industrial sludge produced from textile and leather industrial wastewater

Mostafa Abdul Wahab[1] · Funda Ates[2] · Eyup Yildirir[3] · Norbert Miskolczi[4]

Received: 8 July 2021 / Revised: 1 December 2021 / Accepted: 2 December 2021 / Published online: 13 January 2022

Abstract

This paper elucidates catalytic and non-catalytic pyrolysis characteristics of sludge obtained from the biological treatment of textile and leather industrial wastewater. Iso-conversional model-free methods, such as Flynn–Wall–Ozawa (FWO), Kissinger–Akahira–Sunose (KAS) and Friedman, were employed to evaluate the kinetic and thermodynamic parameters. The E_a (activation energy) values of non-catalytic and catalytic pyrolysis with y-zeolite and activated alumina (Al_2O_3) were determined via KAS method to be in the range of 84.66–291.18, 73.12–197.17 and 84.66–217.44 kJ/mol, respectively, whereas similar trends were observed when the other two methods were used. Gas chromatography/mass spectrometer (GC/MS) analyses showed that the oil obtained from the non-catalytic procedure was rich in fatty acids, steroidal compounds and N-compounds. Activated alumina was effective in removing nitrogen-containing compounds from the oil while y-zeolite promoted deoxygenation and deacidification reactions and, as a result, the oil became rich in alkanes and alkenes which improved its quality as a fuel.

Keywords Sludge · Fast pyrolysis · Thermo-gravimetric analysis · Iso-conversional methods · GC/MS

1 Introduction

Establishing sustainable processes to produce energy from waste and biomass is vital for the proposed circular economy, especially with increasing concerns over the effects of fossil fuels on climate change and global warming. Recently, utilizing biomass and organic waste as a resource for clean energy production has gained much attention. Sludge, as a by-product of the biological treatment of industrial or municipal wastewater, has great potential as organic waste since the amount of wastewater produced globally is nearly 330 km^3/year, which is the source for the sludge [1]. Depending on the type of the wastewater processed, it may contain hazardous and toxic compounds; hence, the disposal of the sludge is important as it may create risks to the environment if it is not handled correctly. In developing countries especially, the amount of sludge has increased dramatically in recent years. In the European Union alone, the total sewage sludge production was recorded as 9.2 million tonnes in 2010, and Turkey's share is around 0.6 million tonnes of sludge annually [2]. Mainly consisting of toxic and hazardous organic compounds, sludge could contain inorganic compounds, such as heavy metals and pathogenic

Highlights
- the E_a of sludge pyrolysis were in the range of 170.63 to 182.77 kJ/mol.
- the calorific value of oil increased from 21.68 to 34.1 MJ/kg via y-zeolite addition.
- Both catalysts reduced the fatty acid content and increased the quality of the oil

✉ Eyup Yildirir
eyup.yildirir@usak.edu.tr

1 Graduate School of Sciences, Iki Eylul Campus, Eskisehir Technical University, Eskişehir, Turkey

2 Department of Chemical Engineering, Faculty of Engineering, Eskisehir Technical University, Iki Eylul Campus, Eskişehir, Turkey

3 Department of Chemical Engineering, Faculty of Engineering, Usak University, Usak, Turkey

4 Institute of Chemical Engineering and Process Engineering, MOL Department of Hydrocarbon & Coal Processing, Faculty of Engineering, University of Pannonia, Veszprem, Hungary

compounds which are major threat to the environment and human health [3]. Therefore, management of sludge is crucial for a sustainable environment and the economy.

Current conventional treatment and disposal methods of sludge consist of landfilling, incineration and agricultural usage [4]. However, there is an increasing concern about these disposal methods due to their contribution to soil and water pollution in relation to the high amount of organic and inorganic toxic compounds in the sludge. As an alternative route, converting the sludge into fuel via thermochemical processes has been widely investigated. One of the most promising methods is the pyrolysis of sludge to produce liquid fuel [5]. Bio-oil as a source of valuable chemicals or fuel with high calorific value could be obtained especially via fast pyrolysis of biomass and organic waste [6]. The fast pyrolysis of sewage sludge has been extensively studied, and the results have proven that the sludge amount decreases tremendously by converting it into liquid and gas products. However, the obtained liquid (bio-oil) has poor quality in terms of calorific value, water content, stability and oxygen content [7]. The bio-oil quality and the selectivity of the products could be enhanced by utilizing catalysts and/or modifiers. Several catalysts have been used in the past, such as KCl, Na_2CO_3, Fe_2O_3, CaO, activated alumina (Al_2O_3), HZSM-5 zeolite and steam as modifiers to increase the yield of the pyrolysis and the quality of bio-oil [8, 9].

Thermo-gravimetric analysis (TGA) is a widely used technique to investigate the kinetics of the thermal decomposition process of solids. Knowing the kinetics of the mass loss of any material throughout their thermal decomposition is essential for characterization, new system development, feasibility assessment and design purposes [10, 11]. Biomass thermal decomposition kinetic parameters could be determined by two techniques: model fitting and iso-conversional methods. Iso-conversional methods are more favourable as, according to Sanchez-Jimenez et. al., model fitting methods could yield uncertainties during the estimation of kinetic parameters and not represent the real case for a process [12]. The Friedman differential method [13], the Flynn–Wall–Ozawa linear integral method [14, 15] and the Kissinger–Akahira–Sunose linear integral method [16] are the most referred iso-conversional methods, due to their simplicity and high accuracy. Many kinetic and thermodynamic parameters, such as activation energy, pre-exponential value, activation enthalpy change, activation Gibbs free energy and activation entropy change, can be obtained using the aforementioned methods by making use of transition state theory (active complex theory) [17].

Especially in developing countries such as Turkey, Bangladesh, Tanzania and South Africa, textile and leather industries are considered as one of the most important economy drivers. In general, low technology for production and waste management is available, and hence, the produced wastes contain vast amounts of toxic and hazardous materials [18]. Due to the nitrogenous contaminants arising from the usage of azo-dyes and extensive usage of chromium during the tanning process, the produced sludge from these industries differs from the sewage and other industrial sludges. In this regard, as pyrolysis enables the routes not only producing liquid fuel, but also potential recovery of resources, it can be a commercially available technology for a sustainable solution [19]. Although pyrolysis of sewage sludge has been investigated in detail, there is very limited data on the pyrolysis of this kind of industrial sludge. The obtained oil could be enhanced with the catalyst addition, and also determination of the kinetic data could contribute to the literature in order to construct a commercial process, since there is not much research on the detection of kinetic parameters for catalytic thermal degradation of textile and leather industrial wastewater sludge in the presence of y-zeolite and Al_2O_3.

In the current study, the thermal kinetic parameters of sludge, obtained from the biological treatment of textile and leather industrial wastewater, were estimated with the help of TGA analysis. Three different model free (iso-conversional) methods, Flynn–Wall–Ozawa (FWO), Kissinger–Akahira–Sunose (KAS) and differential Friedman, were used to determine the activation energy, pre-exponential factor, enthalpy, Gibbs energy and entropy change of activation during the pyrolysis of the sludge. The effects of y-zeolite and an Al_2O_3 catalyst on the activation energy during the thermal degradation of the sludge were also examined. In addition, the effects of y-zeolite and Al_2O_3 as catalysts on the product quality were tested in a fixed bed reactor. The liquid products were analysed via gas chromatography/mass spectrometer (GC/MS) analyzer and the catalytic effects were determined on the oil composition.

2 Materials and methods

2.1 Properties of sludge

The sludge sample was gathered from the Leather and Textile Industry Wastewater Treatment Plant, Uşak, Turkey. Initially, the sludge contained almost 70 wt% of water and, therefore, it underwent a drying process at 110 ℃ for 24 h and was then ground into small particles to yield a particle size distribution of 0.6 mm < D_p < 0.85 mm. The proximate, ultimate and ICP/MS (inductively coupled plasma/mass spectrometry) analysis results and the calorific value of the sludge are given in Table 1. A Thermo-scientific Flash Smart elemental analyzer was used to determine the weight fractions of carbon, hydrogen and nitrogen, with the weight fraction of oxygen being calculated by difference. The HHV (higher heating value) was determined using the Dulong formula [20]. The ICP/MS analysis of

the sludge sample was conducted according to the EPA 6020A method [21].

Y-zeolite was purchased from Zeolyst having the following properties: SiO_2/Al_2O_3 mole ratio = 5.1; nominal cation form: hydrogen; Na_2O content = 2.8 wt%; and a surface area = 730 m^2/g. Activated alumina having a particle size of less than 150 mesh, pore size of 58 Å and a surface of 205 m^2/g was purchased from Sigma-Aldrich.

A Philips MiniPal PW 4025/02 non-polarized energy-dispersive X-ray spectrometer (Philips Co., Alameno, Netherlands, PW 4051 MiniPal/MiniMate Software V 2.0A) was used for the analysis of biochar obtained from the pyrolysis process. The instrument was equipped with a rhodium side-window tube anode and an Si-PIN detector as well as a beryllium window. A helium (99.996% purity) atmosphere was used during the analysis.

2.2 TGA and kinetic analysis

A thermo-gravimetric analyzer (Perkin Elmer Simultaneous Thermal Analyzer, STA 6000) coupled with differential thermal analyzer (DTA) was used. A sample of between 10 and 15 mg was placed in an alumina crucible and heated from 30 to 800 ℃ under a nitrogen atmosphere with a flow rate of 50 ml/min for each analysis. In the catalytic thermo-gravimetric experiments, sludge and the catalyst (10 wt%) were mixed mechanically, then the mixture was ground to obtain a uniform sludge and catalyst mixture samples. Heating rates of 5, 10, 15 and 20 ℃/min were used for the thermal decomposition of the sludge for kinetic parameters' calculations. At least two repetitions were conducted to confirm the accuracy of the results.

2.2.1 Iso-conversional kinetic model

The kinetic models applied in thermal degradation are in general accurate for single reactions. However, for processes including multiple reactions such as sludge pyrolysis, iso-conversional method yields better fit to the experimental data [22]. In this study, Flynn–Wall–Ozawa (FWO) [14, 15], Kissinger–Akahira–Sunose (KAS) [23] and Friedman [13] kinetic models are utilized as iso-conversional methods. By making use of these methods, activation energies for the sludge pyrolysis were determined. The application of the kinetic models is described in Table S1, in Supplementary information section.

2.2.2 Thermodynamic properties

The change in enthalpy, Gibbs free energy and entropy of activation could be obtained with the following formulas:

$$\Delta^o H^{\ddagger} = E_a - RT \tag{1}$$

$$\Delta^o G^{\ddagger} = E_a + RT_p ln\frac{K_B T_p}{hA} \tag{2}$$

$$\Delta^o S^{\ddagger} = \frac{\Delta^o H^{\ddagger} - \Delta^o G^{\ddagger}}{T_p} \tag{3}$$

where K_B is Boltzmann constant (1.3807×10^{-23} J.K^{-1}), h is Planck constant (6.6261×10^{-34} J.s) and T_P is the peak temperature.

Table 1 Proximate, ultimate and ICP/MS analyses and HHV of sludge

Proximate analysis[a] (wt%)		Ultimate analysis[b] (wt%)		ICP/MS analysis (ppm)		HHV (MJ/kg)
Volatiles	43.1	C	45.63	Al	32,652	12.88
Fixed C	15.8	H	3.51	Cr	13,821	
Ash	32.3	N	6.04	Na	9456	
Moisture	8.8	O	43.10	Mg	6636	
		S	1.72	Ca	5777	
				Fe	5190	
				K	2657	
				Sr	189	
				Ba	159	
				Mn	153	
				Zn	121	

[a]Dry basis

[b]The results are expressed as dry, ash-free

2.3 Experimental procedure for pyrolysis and product analysis

The pyrolysis of sludge was carried out in a fixed bed, thin tubular reactor at a pyrolysis temperature of 500 ℃ and at a heating rate of 500 ℃/min under nitrogen atmosphere. The temperature was controlled by an automatic temperature controller. The process setup involves steel wool for fixing 3 g of the sludge sample and catalysts (10 wt%) in case of catalytic runs, a thermocouple inserted into the reactor from the top and fixing flanges at the top and bottom of the reactor for sealing. Two designs were used in this study: catalytic and non-catalytic models as shown in Fig. 1. For the non-catalytic model experiments, steel wool was placed at a height of 20 cm from the bottom of the reactor using an iron rod, with the sludge sample being placed above it. In the catalytic model, two separate catalyst beds were prepared to catalyze the volatiles, appropriately. Steel wool, catalyst, and sludge were then loaded into the reactor in sequence, respectively. In total, 3 g of sludge, 0.6 g of steel wool and 0.3 g of catalyst were placed into the reactor.

When the desired temperature was reached, the reactor system was detained to still for 60 s. Non-condensable and condensable products were moved from the reactor with the carrier gas. Condensable volatile products were cooled and condensed in ice-cooled traps and recovered with dichloromethane (DCM) washing, and the aqueous phase was separated from the oil using a separating funnel. The volume of water was measured with the help of a graduated cylinder after the water and oil mixture was separated from the separating funnel. DCM was removed in a rotary evaporator and the remaining liquid was weighed as oil. The solid residual in the tubular reactor was collected and weighted as char product. The gas product was determined by taking the difference. A more detailed description regarding the reactor can be found in our previous study [24].

All of the yields were calculated on a dry and ash-free (daf) basis, and at least two repetitions were conducted to confirm the accuracy of the results for each experiment. Therefore, each experimental condition and reproducibility of the experiment data was calculated to be within ± 2%.

2.4 Product analysis

The elemental compositions (CHNS/O) of the sludge char and oils were determined with the help of a Perkin Elmer 2400 Series II elemental analyzer. Higher heating value (HHV) of char and oils were determined according to Dulong's formula [20]. BET (Brunauer–Emmett–Teller) analyses were performed with a Quantachrome Touch-Win branded device to determine the surface area of the obtained char.

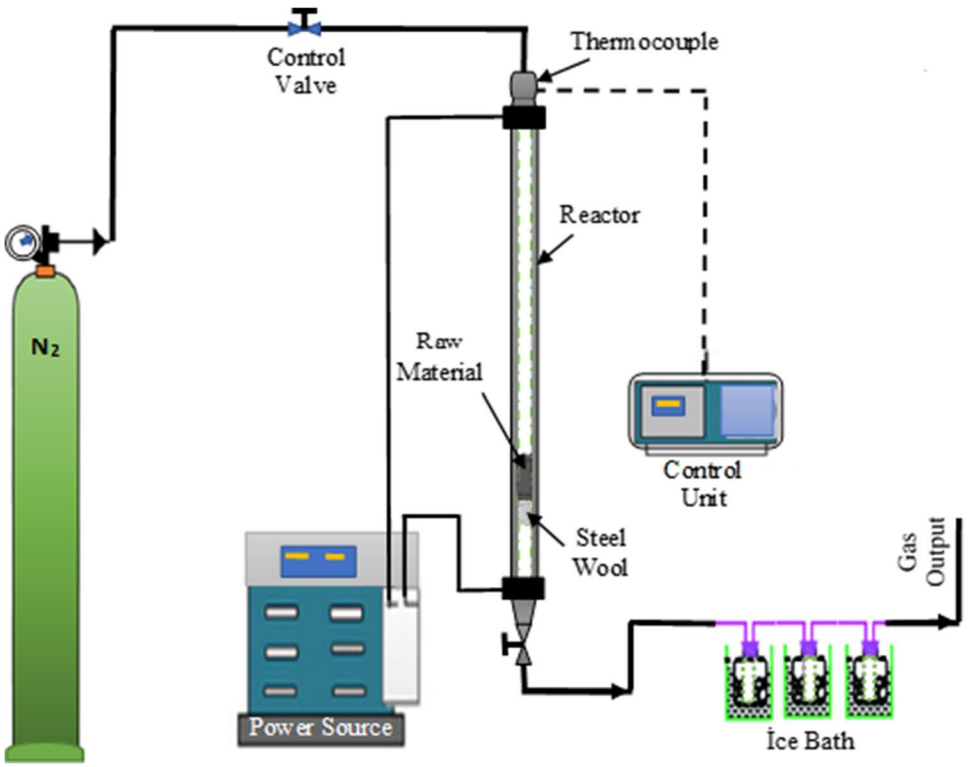

Fig. 1 The experimental setup for pyrolysis of the sludge

An oil analysis was carried out at a constant pyrolysis temperature of 500 ℃ to identify the oil structure. A 7890A/5975C gas chromatography/mass spectrometer (GC/MS) instrument (Agilent, USA) was used to analyse the oil. Initially, the oil obtained from the traps was diluted in DCM for testing by GC/MS and it was then injected into vials which were put into an auto-injector port with an eight-vial capacity. A detailed description of this method can be found elsewhere [25].

3 Results and discussion

3.1 Thermal decomposition of the sludge at different heating rates

The thermal decomposition behaviour of sludge under an N_2 atmosphere from ambient temperature to 800 °C was investigated at heating rates of 5, 10, 15 and 20 ℃/min. The resulting TG and DTG thermographs are shown in Fig. 2a, b, respectively, and indicate that the thermal decomposition of the sludge could be classified in three main stages: dehydration (stage 1), degradation of volatiles (stage 2) and decomposition of carbonaceous materials (stage 3) as summarized in Table S2 in Supplementary information part, together with the initial and final temperatures (T_i and T_f), peak temperatures (T_{m1} and T_{m2}) and the mass losses for pyrolysis of sludge at different heating rates.

The weight loss during the pyrolysis of sludge in stage 1 was mainly due to the moisture content of the sludge and was observed between the ambient temperature and 180–210 °C, for all heating rates. The organic constituents of the sludge, such as proteins, lipids and carbohydrates, started to degrade in stage 2. Two major peaks were detected in the DTG curve: one at the range of 305 and 332 °C, representing the degradation of proteins and carbohydrates, and the other at between 444 and 465 °C, showing the decomposition of lipids [26]. In last stage, the decomposition of carbonaceous materials started and the weight loss occurred.

The total weight loss during the pyrolysis of the sludge did not vary noticeably with the changing heating rates and remained in the range of 69.72 to 66.54 wt%. Similarly, the mass losses at the stages were close to each other as shown in Table S2. However, the peak temperatures T_{m1} and T_{m2} increased with the increasing heating rate; as in stage 2, they were 306.55 and 444.03 ℃ at 5 ℃/min heating rate and became 331.36 and 464.66 ℃ at 20 ℃/min heating rate,

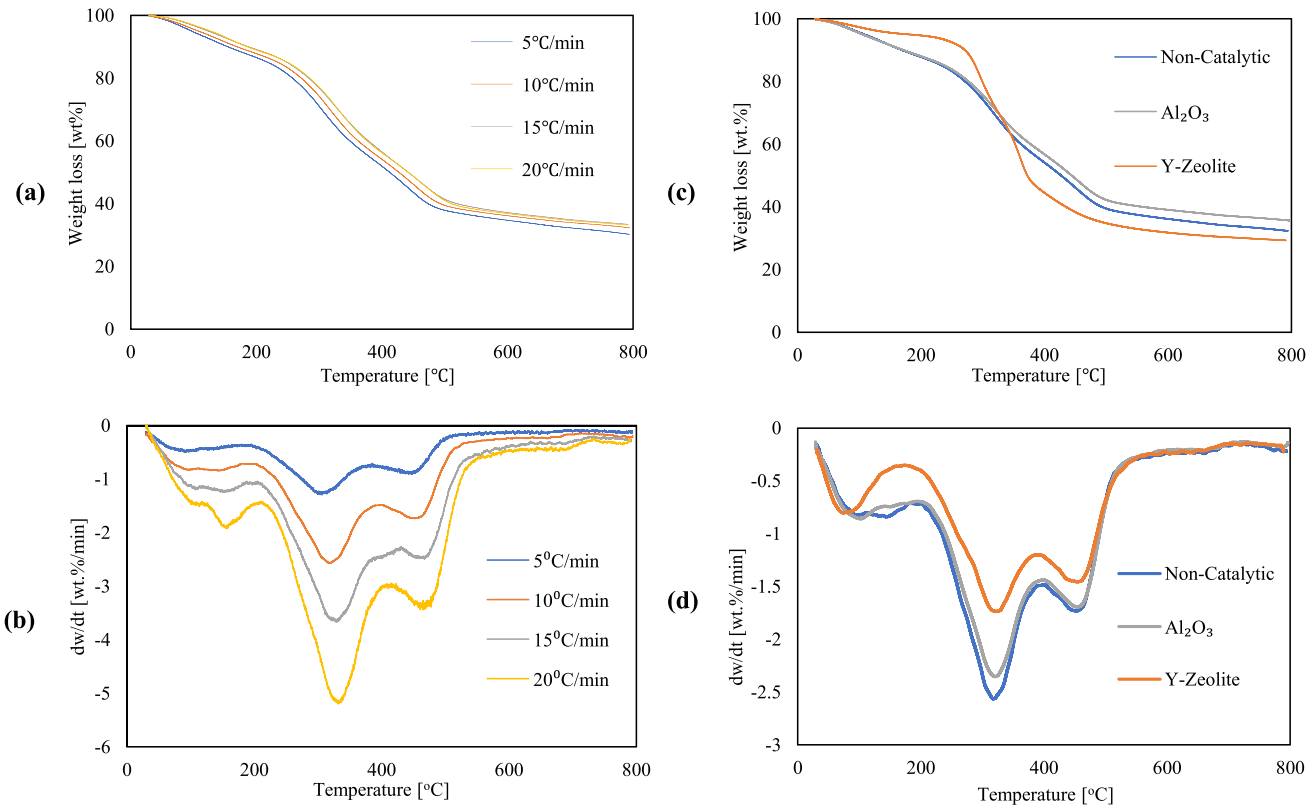

Fig. 2 **a** TG and **b** DTG thermographs for sludge pyrolysis at various heating rates. **c** TG and **d** DTG thermographs for non-catalytic and catalytic sludge pyrolysis at constant heating rate of 10 °C/min

respectively. The peak temperatures in stage 2 indicate the temperatures at which the main pyrolysis reactions take place, hence showing that at lower heating rates, lower temperatures were required for the pyrolysis.

Therefore, increasing the heating rate would increase the energy demand of the pyrolysis process for sludge degradation. In addition, increasing heating rates shifted the boundaries of the stages to higher temperatures as well as peak temperatures. Similar effects are reported in studies with sludge and the compost of sludge during pyrolysis at different heating rates [27–29].

3.2 The effect of catalysts on the thermal decomposition of the sludge

The thermal decomposition behaviour of sludge from ambient temperature to 800 °C was investigated at a constant heating rate of 10 ℃/min and all data is tabulated in the Table S3 in Supplementary information section. The effects of Al_2O_3 and y-zeolite as catalysts were also determined and the resulting TG and DTG thermographs are shown in Fig. 2c, d. The addition of catalysts greatly affected the thermal decomposition rate of the sludge.

The catalytic effect of y-zeolite during the pyrolysis of the sludge was discrete compared to the catalytic effect of Al_2O_3, particularly in stage 1, where different thermal decomposition behaviour were observed. Sludge with y-zeolite yielded much less weight loss compared to other cases which could be a result of the zeolite's capacity to adsorb water, even at low and moderate temperatures. Zeolites are used in low- and medium-temperature air-drying processes due to their ability to remove water from fresh air [30].

The change in the maximum degradation rates also indicates the catalytic effects of Al_2O_3 and y-zeolite, since there was a certain decrease in -DTG (wt%/min) values compared to the non-catalytic pyrolysis. This can also be observed in Fig. 2d as the peak heights in stage 2 lowered in the catalytic cases. As a summary, it could be concluded that both catalysts affected the degradation rates and lowered the required energy for the pyrolysis of the sludge.

3.3 Kinetic and thermodynamic analysis

The kinetic plots for all of the methods were drawn in order to carry out the calculation of kinetic and thermodynamic parameters, and a sample plot for the non-catalytic pyrolysis of sludge is shown in Fig. 3 and plots for catalytic pyrolysis are included in the Supplementary information section as Figures S1 and S2. Activation energies (E_a) were calculated from corresponding slopes of each line drawn for conversion degrees (α) from 0.1 to 0.8, with the correlation coefficients (R^2) for all cases being above 0.93, proving the high accuracy of the kinetic models. All values of the activation energies and pre-exponential factors (A) per conversion degree, for all cases calculated from the corresponding slopes of the kinetic plots, are shown in Table 2. The determined average activation energy values for non-catalytic pyrolysis were 182.77, 170.63 and 175.84 kJ/mol according to the KAS, FWO and Friedman models, respectively. In these methods, the thermal degradation of the solid is defined as a single reaction and small differences in the calculated activation energies by different kinetic models could be a result of this approach, as seen in pyrolysis of biomass and biomass constituents, such as cellulose, hemicellulose and lignin [31–33].

Kinetic modelling of sewage sludge was investigated and a model fitting method was applied in various articles which consider the sludge as two or more pseudo-components. The activation energy, depending on the degree of conversion in these studies, was roughly within the range of 100 to 400 kJ/mol [34–37]. In all of the methods, activation energy and

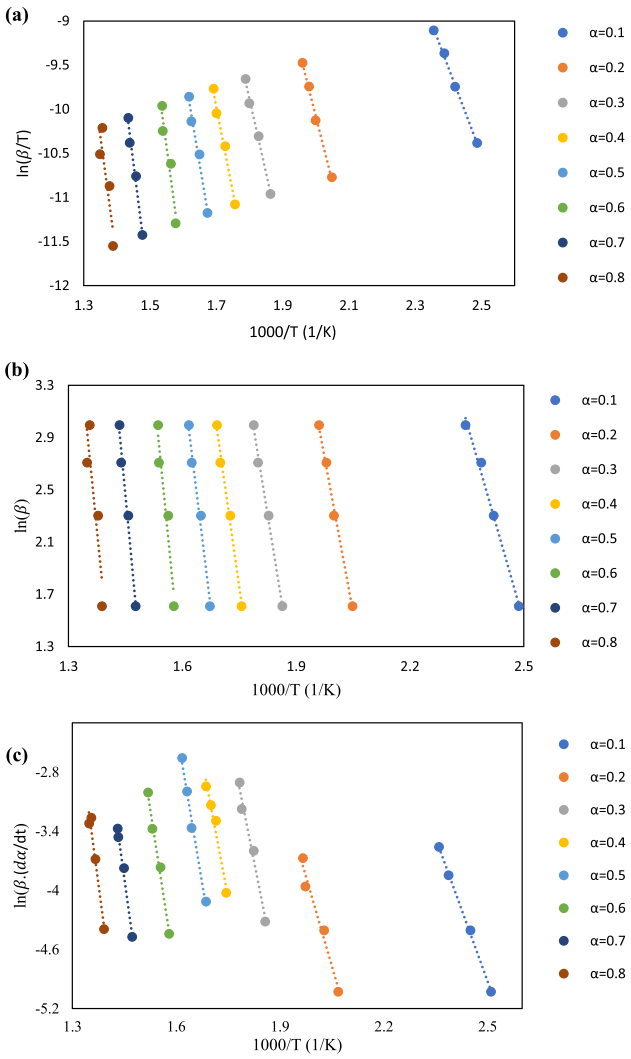

Fig. 3 Kinetic plots of **a** KAS, **b** FWO and **c** Freidman model for non-catalytical pyrolysis of sludge

Table 2 Kinetic parameters for the pyrolysis of sludge via the KAS, FWO and Friedman models

		KAS			FWO			Freidman		
	α	E_a [kJ/mol]	A [s^{-1}]	R^2	E_a [kJ/mol]	A [s^{-1}]	R^2	E_a [kJ/mol]	A [s^{-1}]	R^2
Sludge	0.1	84.66	7.05×10^{06}	0.9980	84.43	6.71×10^{06}	0.9977	90.38	2.38×10^{07}	0.9821
	0.2	123.11	2.33×10^{10}	0.9944	124.25	2.96×10^{10}	0.9960	128.47	7.16×10^{10}	0.9872
	0.3	139.45	7.07×10^{11}	0.9937	140.48	8.76×10^{11}	0.9941	152.23	1.01×10^{13}	0.9959
	0.4	161.27	6.58×10^{13}	0.9888	161.63	7.08×10^{13}	0.9894	130.36	1.06×10^{11}	0.9959
	0.5	186.54	1.22×10^{16}	0.9815	185.96	1.09×10^{16}	0.9823	203.41	3.97×10^{17}	0.9331
	0.6	232.09	1.45×10^{20}	0.9300	229.59	8.66×10^{19}	0.9338	246.41	2.74×10^{21}	0.9733
	0.7	243.87	1.63×10^{21}	0.9798	241.42	9.84×10^{20}	0.9999	209.92	1.52×10^{18}	0.9254
	0.8	291.18	2.63×10^{25}	0.9517	292.68	3.57×10^{25}	0.9999	245.43	2.24×10^{21}	0.9629
	Avg	**182.77**			**170.63**			**175.83**		
Sludge + Al_2O_3	0.1	84.66	7.05×10^{06}	0.9974	84.43	6.71×10^{06}	0.9977	70.51	3.41×10^{05}	0.9547
	0.2	73.93	7.11×10^{05}	0.9990	77.78	1.62×10^{06}	0.9991	94.23	5.37×10^{07}	0.9361
	0.3	104.65	4.85×10^{08}	0.9948	107.63	9.08×10^{08}	0.9957	116.63	6.01×10^{09}	0.9949
	0.4	141.88	1.17×10^{12}	0.9784	143.37	1.60×10^{12}	0.9811	120.21	1.27×10^{10}	0.9968
	0.5	110.30	1.59×10^{09}	0.9743	113.68	3.24×10^{09}	0.9784	125.09	3.53×10^{10}	0.9760
	0.6	142.10	1.23×10^{12}	0.9852	144.41	1.99×10^{12}	0.9871	155.78	2.10×10^{13}	0.9881
	0.7	217.44	7.13×10^{18}	0.9999	216.52	5.89×10^{18}	0.9999	184.89	8.71×10^{15}	0.9395
	0.8	212.42	2.54×10^{18}	0.9999	216.96	6.46×10^{18}	0.9999	192.24	3.97×10^{16}	0.9361
	Avg	**135.92**			**129.31**			**132.45**		
Sludge + y-zeolite	0.1	73.12	5.98×10^{05}	0.9652	64.05	8.44×10^{04}	0.9712	69.66	2.48×10^{05}	0.9622
	0.2	77.04	1.38×10^{06}	0.9387	80.59	2.96×10^{06}	0.9491	94.01	5.12×10^{07}	0.8760
	0.3	102.40	3.02×10^{08}	0.9847	105.43	5.72×10^{08}	0.9869	104.99	5.21×10^{08}	0.9951
	0.4	115.73	4.97×10^{09}	0.9761	118.59	9.05×10^{09}	0.9795	121.58	1.69×10^{10}	0.9891
	0.5	129.36	8.62×10^{10}	0.9491	131.97	1.49×10^{11}	0.9558	137.73	4.94×10^{11}	0.9058
	0.6	127.71	6.10×10^{10}	0.9907	130.91	1.19×10^{11}	0.9920	156.99	2.71×10^{13}	0.9897
	0.7	162.24	8.03×10^{13}	0.9999	164.23	1.21×10^{14}	0.9999	167.74	2.51×10^{14}	0.9529
	0.8	197.17	1.10×10^{17}	0.9999	202.21	3.10×10^{17}	0.9999	180.34	3.40×10^{15}	0.9502
	Avg	**123.10**			**117.78**			**129.13**		

pre-exponential factor values increased with an increasing conversion degree. Similar trends were observed in other reports in the literature investigating the kinetics of pyrolysis of leather waste and biomass samples [38, 39].

The pre-exponential factors for non-catalytic pyrolysis of sludge ranged from 10^6 to 10^{25} according to all kinetic models. While the high values of pre-exponential factor indicate that numerous chemical reactions were taking place during the pyrolysis of sludge, the wide range of the values shows the complex structure of the sludge, since A is defined as the degree of collision of a reaction per unit time [40].

The presence of Al_2O_3 and y-zeolite affected the values of both the activation energy and pre-exponential factor values. According to all methods used, the average activation energy decreased during the catalytic pyrolysis of the sludge showing that both catalysts were effective. Although the values of the pre-exponential factor decreased slightly, they were still ranged high between 10^6 and 10^{18} s^{-1}.

The changes in enthalpy, Gibbs free energy and entropy of activation as thermodynamic parameters were determined for the pyrolysis of the sludge, and all values per conversion degree are shown in Table 3. The activation enthalpy change values with the changing conversion degree were positive, showing that the reactions occurring during pyrolysis were endothermic. In addition, while the enthalpy increased with the increasing conversion degree, the difference between E_a and $\Delta^o H^{\ddagger}$ was around 5 kJ/mol, indicating that product formation was easily achievable [41]. The catalyst addition decreased the $\Delta^o H^{\ddagger}$ values, whereas y-zeolite was more effective since the decrease was more discrete.

Gibbs free energy represents the increase in the total energy of a system necessary for the development of an activated complex [42]. The $\Delta^o G^{\ddagger}$ values were in an extremely narrow range and slightly increased with the increasing conversion degree, and were between 156.2 and 150 kJ/mol, according to all three kinetic models.

Entropy changes at conversion degrees of less than 0.3 were negative during the non-catalytic pyrolysis and it remained negative until the conversion degree reached 0.6 in the presence of catalysts according to the KAS and FWO models. The

Table 3 Thermodynamic parameters for the pyrolysis of sludge via the KAS, FWO and Friedman models

		KAS			FWO			Freidman		
	α	$\Delta^o H^{\ddagger}$[kJ/mol]	$\Delta^o G^{\ddagger}$[kJ/mol]	$\Delta^o S^{\ddagger}$[kJ/mol.K]	$\Delta^o H^{\ddagger}$[kJ/mol]	$\Delta^o G^{\ddagger}$[kJ/mol]	$\Delta^o S^{\ddagger}$[kJ/mol.K]	$\Delta^o H^{\ddagger}$[kJ/mol]	$\Delta^o G^{\ddagger}$[kJ/mol]	$\Delta^o S^{\ddagger}$[kJ/mol.K]
Sludge	0.1	79.69	156.21	− 127.92	79.46	156.22	− 128.33	85.41	155.88	− 117.81
	0.2	118.13	154.34	− 60.54	119.28	154.30	− 58.54	123.50	154.13	− 51.21
	0.3	134.48	153.72	− 32.18	135.51	153.69	− 30.39	147.26	153.29	− 10.08
	0.4	156.30	153.00	5.51	156.66	152.99	6.13	125.38	154.06	− 47.94
	0.5	181.57	152.28	48.97	180.99	152.29	47.98	198.44	151.85	77.89
	0.6	227.12	151.19	126.94	224.62	151.24	122.66	241.44	150.89	151.38
	0.7	238.90	150.94	147.04	236.45	150.99	142.87	204.95	151.69	89.04
	0.8	286.21	150.06	227.61	287.71	150.04	230.17	240.46	150.91	149.70
Sludge + Al_2O_3	0.1	79.69	156.21	− 127.92	79.46	156.22	− 128.33	65.54	157.12	− 153.10
	0.2	68.96	156.88	− 146.99	72.81	156.63	− 140.13	89.26	155.67	− 111.04
	0.3	99.68	155.15	− 92.74	102.66	155.01	− 87.53	111.66	154.61	− 71.82
	0.4	136.91	153.64	− 27.97	138.40	153.59	− 25.39	115.23	154.46	− 65.59
	0.5	105.33	154.89	− 82.86	108.71	154.74	− 76.96	120.12	154.26	− 57.09
	0.6	137.12	153.63	− 27.60	139.44	153.55	− 23.59	150.80	153.17	− 3.97
	0.7	212.47	151.52	101.90	211.54	151.54	100.32	179.92	152.32	46.13
	0.8	207.45	151.63	93.32	211.99	151.53	101.09	187.27	152.13	58.75
Sludge + y-zeolite	0.1	68.15	156.93	− 148.43	59.07	157.59	− 164.71	64.69	157.18	− 154.63
	0.2	72.07	156.68	− 141.45	75.62	156.45	− 135.14	89.04	155.69	− 111.43
	0.3	97.43	155.26	− 96.69	100.46	155.11	− 91.37	100.02	155.14	− 92.15
	0.4	110.76	154.65	− 73.39	113.61	154.53	− 68.41	116.61	154.41	− 63.19
	0.5	124.39	154.10	− 49.67	127.00	154.00	− 45.13	132.76	153.79	− 35.16
	0.6	122.73	154.16	− 52.54	125.94	154.04	− 46.98	152.02	153.14	− 1.87
	0.7	157.26	152.97	7.17	159.25	152.91	10.60	162.77	152.81	16.65
	0.8	192.20	152.00	67.20	197.24	151.88	75.84	175.36	152.45	38.32

Friedman model suggests that in non-catalytic pyrolysis, ΔS remains constant for conversion degree of less than 0.4, and in catalytic pyrolysis, at conversion degrees higher than 0.7, $\Delta^o S^{\ddagger}$ becomes positive. The negative values of $\Delta^o S^{\ddagger}$ indicate that the produced substances are more organized in molecular structure compared to the initial substances, showing that before reaching the thermo-dynamic equilibrium, substances undergo a chemically or physically ageing process [43]. Therefore, it can be concluded that the addition of a catalyst enhances the production of substances with more organized molecular structure.

3.4 The effect of catalysts on product yields

The sludge gathered from leather and textile industrial wastewater treatment plants was low in volatiles and rich in inorganic matter, as listed in Table 1, compared to sewage sludge samples studied by various researchers [5, 44–49]. The high inorganic content and low fraction of volatiles influence the reaction routes to produce more gas and/or char during the pyrolysis. It is known that high ash in the feed can have a catalytic effect and promote gas formation via cracking reactions and char formation via carbonization reactions [50]. The same effect is observed in this study as oil yield was 24.7% during the non-catalytic pyrolysis while it was in the range of 40 to 50% in studies of sewage sludge pyrolysis.

In general, water is produced via dehydration of the organic substances or the moisture of the sample feed could be responsible during the pyrolysis. Water obtained during the non-catalytic pyrolysis of sludge was 7.2 wt% which is lower than the initial moisture content of the sludge (8.8 wt%). This could indicate that some water was consumed during the pyrolysis [4, 51]. The inorganic content of the sludge could promote the water–gas (4) and water–gas shift (5) reactions, and hence, water could be consumed through these reactions.

$$C + H_2O \rightarrow CO + H_2 \tag{4}$$

$$CO + H_2O \rightarrow CO_2 + H_2 \tag{5}$$

The catalytic pyrolysis yielded slightly higher water as they were 8.3 wt% and 8.1 wt% for y-zeolite and Al_2O_3, respectively.

The product distribution during the non-catalytic and the catalytic pyrolysis of the sludge showed that all product yields were affected when catalysts were used during the pyrolysis (Fig. 4). The oil yield slightly increased from 24.7 to 25.8%, as well as the gas yield, in the presence of Al_2O_3. The intermediates produced with thermal cracking underwent a sequence of aromatization, alkylation and isomerization reaction on the catalyst surface to create aliphatic and aromatic compounds, thereby improving the yield of oil. A similar effect of this catalyst was reported in studies with sewage sludge as oil composition was enhanced with the addition of Al_2O_3 [52, 53]. While the gas yield increased slightly, the char yield decreased suggesting that the presence of Al_2O_3 also promoted the secondary cracking of macromolecular volatile substances formed during the pyrolysis.

The addition of y-zeolite dramatically decreased the oil and char yields, while the gas yield increased. The yields of oil and gas were 24.7 wt% and 25.1 wt%, under non-catalytic pyrolysis, and addition of y-zeolite decreased the oil yield to 20.3 wt% while gas yield increased to 30.0 wt%. As can be seen from the kinetic analysis section, y-zeolite was proven to be more effective in decreasing the activation energy during the pyrolysis of the sludge. The decreasing oil yield in the presence of y-zeolite could be a result of the promotion of cracking and carbonization reactions on the catalyst surface, yielding less oil fraction. The increase in the yields of char and gas products supports this idea. Xie et. al. reported the same effect of zeolite, as they used a HZSM-5 catalyst during the pyrolysis of sewage sludge and observed that the yield of oil decreased [44].

3.5 Analysis of oil products

3.5.1 Elemental and heating value analysis of char and oils

Table 4 compares the elemental analysis and the higher heating values (HHV) of the char and oils obtained from pyrolysis of sludge at a pyrolysis temperature of 500 °C. The char produced from non-catalytic pyrolysis has a higher heating value of 28.3 MJ/kg and surface area is 17.37 m^2/g showing that it can act as a fuel substitute or be evaluated to produce activated carbon. The carbon and hydrogen content of the oils increased with the addition of the catalysts. In addition, the utilization of Al_2O_3 catalyst resulted in lower oxygen content of 29.06% and higher heating value of 25.42 MJ/kg. The use of y-zeolite catalyst during pyrolysis produced

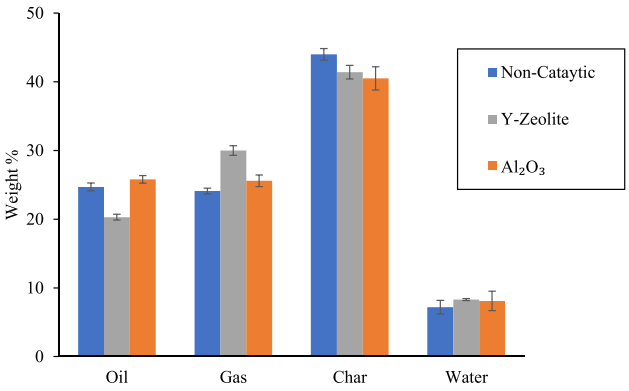

Fig. 4 The product yields during the pyrolysis of sludge

highly deoxygenated oil (oxygen content of 14.9%) with a high heating value of 34.1 MJ/kg, indicating that it was more effective catalyst since the quality of oil was higher.

The XRF analysis of the char was also performed as shown in Fig. 5. Based on the results, it can be seen that well-separated characteristic peaks are observable in the sample represented: Cl (Kα), C (Kα, Kβ), Sb (Lα, Lβ1, Lβ2), Cr (Kα, Kβ), Mn (Kα, Kβ) and Fe (Kα, Kβ). Quantitative analysis shows 7% chlorine, 32% calcium, 37% chromium, 1% manganese, 16% iron and 7% antimony in the sample for elements with a higher molecular weight that sodium. The previous elements are present in the form of their compounds. The results suggest that the majority of the heavy metals remain in the solid phase during the pyrolysis of the sludge.

Table 4 Elemental compositions and calorific values of the sludge char and oils

	Char without catalyst	Oil without catalyst	Oil with Al_2O_3	Oil with y-zeolite
C	80.4	56.14	63.2	72.4
H	2.5	5.8	6.4	8.5
N	2.1	5.8	0.86	3.8
S	0.71	0.51	0.48	0.39
O	14.29	31.75	29.06	14.91
HHV*	28.29	21.68	25.42	34.10

*HHV (MJ/kg) = higher heating value calculated by Dulong's formula [20] (HHV = $(33.83C + 144.3 \times (H - \frac{O}{8}) + 9.38S)$)

3.5.2 GC/MS analysis of oils

The oils obtained from non-catalytic and catalytic pyrolysis of sludge were analysed using gas chromatography/mass spectroscopy (GC/MS) and the resulting chromatograms are given in Figure S3 in Supplementary information section. All the major peaks in the chromatograms were identified and their relative area percentages were calculated as given in Tables 5, 6 and 7 showing that a detailed component analysis of the oils was carried out. In addition, major components produced from non-catalytic and catalytic pyrolysis are shown in Fig. 6 to observe the catalytic effect on the product distribution.

The oil produced in the absence of any catalysts contained approximately 69.7% fatty acids, 5% N-compounds, 2.8% aliphatics (alkanes and alkenes), 3.1% amides and 3.3% oxygenated phenolic compounds. Steroidal hydrocarbons were also produced, since cholesterol, cholest-5-en-3-ol (3beta), cholesta-3,5-diene and cholest-4-en-3-one were 16.1% of the

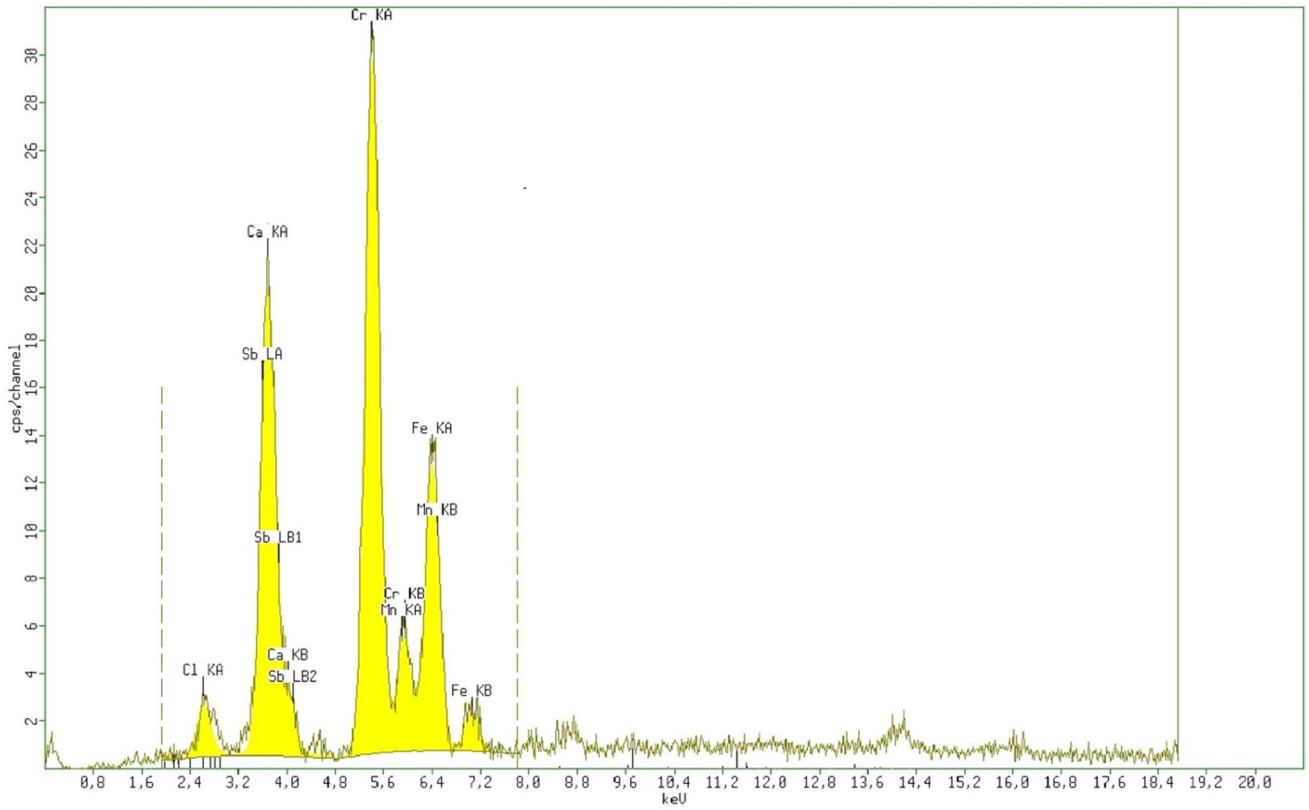

Fig. 5 The X-ray spectra of the char during the pyrolysis of sludge

oil analysed. The wastewater treated in the leather and textile industrial area contains proteinous materials and lipids derived from chromium tanning and pickling processes. The nitrogenous and oxygenated phenolic compounds were likely to be degraded from the protein fraction of the sludge. Fatty acids in the oil are typical thermal degradation products of the lipids and, due to the nature of the sludge being gathered from leather industrial waste, its proportion was high [54]. The presence of the oxygenated phenolic compound can cause the oil to become unstable during long-term storage and transportation. In addition, oil containing N-compounds and amides contributes to the release of the toxic pollutant NO_X during a combustion process. In addition, the high acid content of the oil could reduce the pH, thereby making it corrosive. Therefore, if the oil produced from this sludge were to be used as fuel, a pre-process, such as steam cracking, hydrogenation or Fischer–Tropsch synthesis, should be applied to yield a higher quality of oil with low oxygenated and nitrogenous compounds, as well as low acidity [55].

Table 5 Main and relatively large compounds (area per cent) in oils derived from pyrolysis of sludge without catalyst

Peak number	Retention time (min)	Compound name	Area (%)
1	20.41	1-Tetradecene	1.67
2	23.09	Pentadecane	1.08
3	29.43	Tetradecanoic acid	4.61
4	31.37	Pentadecanoic acid	1.16
5	31.92	Hexadecanenitrile	3.1
6	33.65	Hexadecanoic acid	27.83
7	35.2	Heptadecanoic acid	1.42
8	35.79	Heptadecanenitrile	1.94
9	36.78	9-Octadecenoic acid	25.11
10	37.15	Octadecanoic acid	9.56
11	37.41	Hexadecanamide	3.1
12	37.71	Phenol, 4,4′-(1-methylethylidene)bis	3.3
13	47.58	Cholesterol	1.06
14	48.05	Cholesta-3,5-diene	4.92
15	51.01	Cholest-5-en-3-ol (3beta)	6.73
16	52.84	Cholest-4-en-3-one	1.35
17	54.21	Lanosta-8,24-dien-3-ol (3beta)	2.05

The presence of catalysts during the pyrolysis of sludge alters the vapour phase reaction pathways, changes and improves the liquid product composition. In principle, the use of both catalysts reduced fatty acid content, which is classified as long-chain organic compounds, since it is a carbon distribution of between 13 and 18, and promotes the formation of aliphatic hydrocarbons, such as alkanes and alkenes. Catalysts play an effective role in the cracking of fatty acids [56].

Steroidal hydrocarbons are major compounds in non-catalytic sludge pyrolysis. These compounds are diminished using catalysts. It is thought that the hydrothermal alteration reactions are dominant on the conversion of the steroidals [57].

Nonetheless, the effects of both catalysts on the liquid product are specific in view of the compounds created. Methoxy phenols are abundant in Al_2O_3 studies. Cyclic and aromatic compounds increase with the use of catalysts such as HZSM-5, y-zeolite and activated alumina in pyrolysis compared to non-catalytic procedure [58]. Al_2O_3 had a cracking effect on the liquid components and shortly afterwards a unifying effect. The long-chain fatty acids and steroidal compounds formed in the first stage were broken down and the products developed subsequently merged into methoxy phenols. Fatty acids decreased from 69.7 to 24.6% and steroidal compounds decreased from 16.1 to 2.7% in the presence of a catalyst. While nitrogen-containing

Table 6 Main and relatively large compounds (area per cent) in oils derived from pyrolysis of sludge with Al_2O_3 catalyst

Peak number	Retention time (min)	Compound name	Area (%)
1	12.18	Phenol, 2-methoxy	8.91
2	15.2	Phenol, 2-methoxy-4-methyl	6.23
3	17.6	Phenol, 4-ethyl-2-methoxy-	4.8
4	19.65	Phenol, 2,6-dimethoxy	11.71
5	22.08	Phenol, 2-methoxy-4-(1-propenyl)	16.29
6	23.97	2.3.5-Trimethoxytoluene	4.62
7	25.76	Phenol, 2,6-dimethoxy-4-(2-propenyl)	12.93
8	33.39	Hexadecanoic acid	13.27
9	36.57	9-Octadecenoic acid	7.72
10	36.98	Octadecanoic acid	3.64
11	37.75	Phenol, 4,4′-(1-methylethylidene)bis-	4.93
12	43.09	1–2,Benzenedicarboxylic acid	1.88
13	50.35	Chloest-5-en-3-ol (3beta)	2.73

Table 7 Main and relatively large compounds (area per cent) in oils derived from pyrolysis of sludge with y-zeolite catalyst

Peak number	Retention time (min)	Compound name	Area (%)
1	3.62	Toluene	0.3
2	5.56	Benzene, ethyl-	0.22
3	5.76	p-Xylene	0.28
4	6.27	1-Nonene	0.15
5	6.31	Styrene	0.73
6	6.35	Benzene, 1,2-dimethyl-	0.39
7	6.84	2-Cyclopenten-1-one, 2-methyl-	0.36
8	8.25	Benzene, 1-ethyl-2-methyl-	0.21
9	9.09	1-Decene	0.56
10	9.18	Benzene, 1,2,3-trimethyl	0.42
11	9.33	Decane	0.32
12	9.51	Phenol	0.87
13	12.08	1-Undecene	0.77
14	12.28	Phenol, 4-methyl-	1.68
15	13.8	1-Methylindene	0.58
16	14.81	Naphthalene	1.07
17	15.07	1-Dodecene	2.15
18	15.23	Dodecane	1.32
19	15.38	Dodecane, 4,6-dimethyl	0.32
20	17.6	Phenol, 4-ethyl-2-methoxy-	0.34
21	17.79	1-Tridecene	1.53
22	17.92	Naphthalene, 1-methyl-	0.94
23	18.02	Tridecane	1.09
24	18.38	Naphthalene, 2-methyl-	1.26
25	19.67	Phenol, 2,6-dimethoxy-	0.42
26	20.45	1-Tetradecene	2.04
27	20.71	Tetradecane	1.51
28	21.19	Naphthalene, 1,7-dimethyl-	0.17
29	22.01	1-Tetradecanol	0.64
30	22.62	Cyclododecane	0.31
31	22.78	Trans-7-pentadecene	0.67
32	22.98	1-Pentadecene	3.49
33	23.23	Pentadecane	0.43
34	23.48	Pentadecanol	0.71
35	25.25	1-Hexadecene	2.27
36	25.47	Hexadecane	0.61
39	26.87	Benzene, decyl-	0.44
40	27.16	1-Heptadecene	0.49
41	27.33	Heptadecane	0.77
42	27.61	Tetradecanenitrile	2.61
43	29.43	Tetradecanoic acid	2.69
44	29.64	1-Octadecene	1.07
45	29.86	Octadecane	1.09
46	30.77	1-Nonadecene	0.42
47	30.95	Nonadecane	0.68
48	31.18	Pentadecanoic acid	0.72
49	32	Hexadecanenitrile	9.78
50	33.53	Hexadecanoic acid	6.76
51	35.02	Heneicosene	0.81
52	35.4	Heneicosane	1.7
53	35.5	Heptadecanenitrile	5.75
56	36.98	9-Octadecenoic acid	6.59
57	37.22	Octadecenoic acid	2.78
58	37.59	Hexadecanamide	2.79
59	38.643	4-Methylheptanamide	0.3
60	39.08	1-Tricosene	0.58
61	40.42	Tricosane	1.25
62	40.58	1-Tetracosene	0.4
63	40.81	Tetracosane	1
64	47	Cholesterol	3.49
65	48.15	Cholestadiene	4.43
66	52.87	Cholest-4-en-3-one	1.01

components, such as hexadecanenitrile, heptadecanenitrile and hexadecanamide, were not detected in the presence of Al_2O_3, this catalyst can be described as effective in removing nitrogen-containing components. However, since methoxy phenols as oxygen-containing compounds remained in the oil, Al_2O_3 is not considered to be effective in removing oxygenated compounds from the liquid products.

Zeolites as the most widely used solid acids are aluminosilicate materials with three-dimensional crystalline structure. They are effective to convert oxygenated compounds into hydrocarbons and in catalytic cracking, deoxygenation, dehydration and decarboxylation reactions [59]. Bronsted and Lewis acidic sites are responsible for the cracking effect created by zeolites.

Positive and important changes in the product composition were observed in experiments with y-zeolite. The most obvious effect of the y-zeolite catalyst on sludge decomposition is related to changes in the fatty acid, aliphatics, N-compounds and steroidal compound content of the oil produced. A decrease in fatty acids and increase in aliphatic content were observed while the pyrolysis process was conducted in the presence of the y-zeolite. It was very effective in deacidification reactions, and most hydrocarbons were possibly produced by the conversion of these acids. A major improvement in the oil quality when using y-zeolite was due to the increase of aliphatics and the reduction of fatty acids, which confirms the results reported in the literature. Miskolczi et. al. studied the effect of y-zeolite, β-zeolite and Ni-Mo catalysts on heavy oil and municipal plastic waste and they report that catalysts promote the production of aromatic compounds, while non-catalytic processes do not yield much aromatic reaction [60].

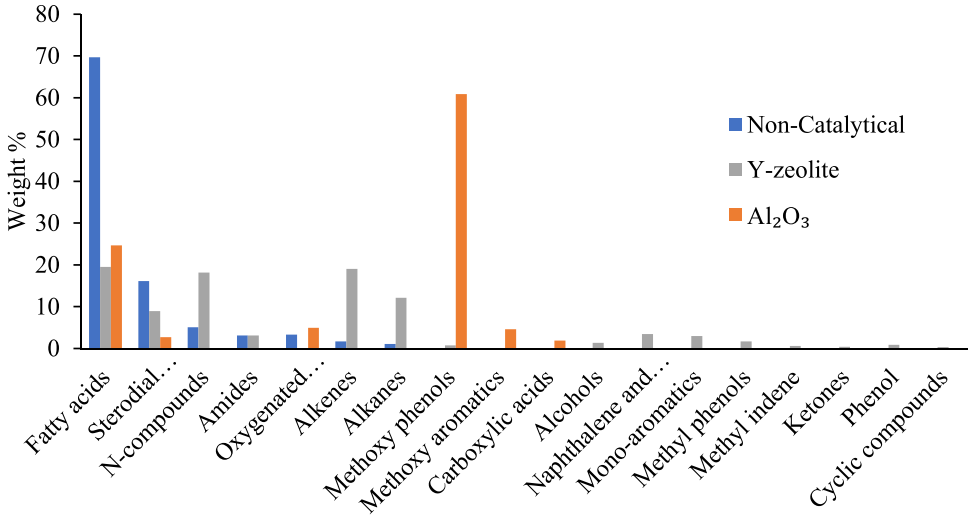

Fig. 6 Classification of pyrolysis oils

The presence of alkanes and alkanes (aliphatic) in the liquid product determines the quality of the fuel. In other words, if the liquid product obtained by pyrolysis contains a significant amount of aliphatic hydrocarbons, it can be evaluated as synthetic fuel. Oil product obtained by the non-catalytic pyrolysis only contained 2.75% aliphatics (C_{14}–C_{15}), whereas in the presence of y-zeolite, aliphatic concentration increased to 31.1%. The formation of lower molecular weight hydrocarbons is dominant during sludge pyrolysis with y-zeolite. The distribution of carbon in the aliphatics is between C_9 and C_{24}, and a more concentrated distribution is between C_{12} and C_{15}. Because the carbon distribution of oil obtained in this study is considered to be between a gasoline (C_5–C_{12}) and diesel (C_9–C_{21}) equivalent, oil obtained via catalytic pyrolysis of sludge in the presence of y-zeolite could be evaluated as fuel.

The formation of mono-ring aromatics, naphthalene and derivatives is another positive improvement in the oil quality with the addition of a catalyst. While mono-ring aromatic components and naphthalene were not observed with the use of Al_2O_3, these organic substances were detected as 3% and 3.4% in the presence of y-zeolite, respectively. The mono-ring aromatic components detected in the oil obtained with y-zeolite included toluene, ethylbenzene, p-xylene, styrene and oxygen-free benzene derivatives (methylbenzene).

Contrary to Al_2O_3, y-zeolite promotes deoxygenation reactions where oxygen is removed in the form of CO_2, CO and H_2O [61]. As a result, methoxy phenols detected in the oil product in the presence of y-zeolite are very low (0.76%) when compared to oil product with Al_2O_3. The results are also in agreement with the elemental analysis results. The percentage of oxygen in the oil product obtained with y-zeolite catalyst was found to be quite low when compared to the Al_2O_3.

N-compounds in the oil during the catalytic pyrolysis via y-zeolite are found to have increased. These components, obtained as 5% in the case of the non-catalytic run, increased by 18.1% with y-zeolite. It was earlier described how y-zeolite forms straight-chain hydrocarbons. The formed N-compounds were nitrogen-bound with straight chains. As a result, y-zeolite can be used as an effective catalyst for the catalytic upgrading of pyrolytic oils.

4 Conclusion

The present study revealed the thermal or catalytic pyrolysis behaviour of industrial sludge, obtained from the Leather and Textile Industry Wastewater Treatment Plant. The catalytic effects of y-zeolite and activated Al_2O_3 on bio-oil compound selectivity were investigated. Extracted from the results of TGA and GC/MS, catalysts had an obvious effect on pyrolysis process, kinetic parameters and oil properties of industrial sludge. Thermal behaviour and thermal degradation kinetic analysis indicated that the use of a catalyst was able to improve the reaction rates during pyrolysis. Catalytic pyrolysis with the use of y-zeolite resulted in a lower average E_a when compared to activated Al_2O_3 or the non-catalytic procedure. Activation energy was reduced from 170.63 to 117.78 kJ/mol, in the presence of y-zeolite. The percentage of oxygen in the oil product obtained with y-zeolite catalyst was found to be quite low when compared to the Al_2O_3. Activated Al_2O_3 could be described as effective in removing nitrogen-containing components; on the other hand, y-zeolite was highly effective in deoxygenation and deacidification reactions. Therefore, the formation of lower molecular weight hydrocarbons was dominant during sludge pyrolysis with y-zeolite.

The results demonstrated that the sludge from the Leather and Textile Industry Wastewater Treatment Plant offers good potential for pyrolysis, and that the oil produced with the use of y-zeolite can be used as a fuel substitute for fossil fuels.

Supplementary Information The online version contains supplementary material available at https://doi.org/10.1007/s13399-021-02183-5.

References

1. Khalid S, ShahidNatasha M et al (2018) A review of environmental contamination and health risk assessment of wastewater use for crop irrigation with a focus on low and high-income countries. Int J Environ Res Public Health 15:895. https://doi.org/10.3390/ijerph15050895
2. Eurostat (2015) Total sewage sludge production from urban wastewater. In: Eurostat. https://ec.europa.eu/eurostat/tgm/table.do?tab=table&plugin=1&language=en&pcode=ten00030. Accessed 5 Mar 2020
3. Xu C, Chen W, Hong J (2014) Life-cycle environmental and economic assessment of sewage sludge treatment in China. J Clean Prod 67:79–87. https://doi.org/10.1016/j.jclepro.2013.12.002
4. Karayildirim T, Yanik J, Yuksel M, Bockhorn H (2006) Characterisation of products from pyrolysis of waste sludge. Fuel 85:1498–1508. https://doi.org/10.1016/j.fuel.2005.12.002
5. Park HJ, Heo HS, Park Y-K et al (2010) Clean bio-oil production from fast pyrolysis of sewage sludge: effects of reaction conditions and metal oxide catalysts. Bioresour Technol 101:S83–S85. https://doi.org/10.1016/j.biortech.2009.06.103
6. Socci J, Saraeian A, Stefanidis SD et al (2019) The role of catalyst acidity and shape selectivity on products from the catalytic fast pyrolysis of beech wood. J Anal Appl Pyrolysis:104710. https://doi.org/10.1016/j.jaap.2019.104710
7. Ma R, Huang X, Zhou Y et al (2017) The effects of catalysts on the conversion of organic matter and bio-fuel production in the microwave pyrolysis of sludge at different temperatures. Bioresour Technol 238:616–623. https://doi.org/10.1016/j.biortech.2017.04.103
8. Yang J, Xu X, Liang S et al (2018) Enhanced hydrogen production in catalytic pyrolysis of sewage sludge by red mud: thermogravimetric kinetic analysis and pyrolysis characteristics. Int J Hydrogen Energy 43:7795–7807. https://doi.org/10.1016/j.ijhydene.2018.03.018
9. Hu Y, Yu W, Wibowo H et al (2019) Effect of catalysts on distribution of polycyclic-aromatic hydrocarbon (PAHs) in bio-oils from the pyrolysis of dewatered sewage sludge at high and low temperatures. Sci Total Environ 667:263–270. https://doi.org/10.1016/j.scitotenv.2019.02.320
10. Font R, Garrido MA (2018) Friedman and n-reaction order methods applied to pine needles and polyurethane thermal decompositions. Thermochim Acta 660:124–133. https://doi.org/10.1016/j.tca.2018.01.002
11. Onsree T, Tippayawong N, Zheng A, Li H (2018) Pyrolysis behavior and kinetics of corn residue pellets and eucalyptus wood chips in a macro thermogravimetric analyzer. Case Stud Therm Eng 12:546–556. https://doi.org/10.1016/j.csite.2018.07.011
12. Sánchez-Jiménez PE, Pérez-Maqueda LA, Perejón A, Criado JM (2013) Limitations of model-fitting methods for kinetic analysis: polystyrene thermal degradation. Resour Conserv Recycl 74:75–81. https://doi.org/10.1016/j.resconrec.2013.02.014
13. Friedman HL (1964) Kinetics of thermal degradation of char-forming plastics from thermogravimetry. Application to a phenolic plastic. J Polym Sci Polym Symp 6:183–195
14. Flynn JH, Wall LA (1966) General treatment of the thermogravimetry of polymers. J Res Natl Bur Stand Sect A Phys Chem 70A:487. https://doi.org/10.6028/jres.070a.043
15. Ozawa T (1965) A new method of analyzing thermogravimetric data. Bull Chem Soc Jpn 38:1881–1886. https://doi.org/10.1246/bcsj.38.1881
16. Kissinger HE (1956) Variation of peak temperature with heating rate in differential thermal analysis. J Res Natl Bur Stand (1934) 57:217. https://doi.org/10.6028/jres.057.026
17. Low PS, Bada JL, Somero GN (1973) Temperature adaptation of enzymes: roles of the free energy, the enthalpy, and the entropy of activation. Proc Natl Acad Sci 70:430–432. https://doi.org/10.1073/pnas.70.2.430
18. Goedhuys M, Janz N, Mohneny P (2014) Knowledge-based productivity in "low-tech" industries: evidence from firms in developing countries. Ind Corp Chang 23:1–23. https://doi.org/10.1093/icc/dtt006
19. Gao N, Kamran K, Quan C, Williams PT (2020) Thermochemical conversion of sewage sludge: a critical review. Prog Energy Combust Sci 79:100843. https://doi.org/10.1016/j.pecs.2020.100843
20. Nzihou JF, Hamidou S, Bouda M et al (2014) Using Dulong and Vandralek formulas to estimate the calorific heating value of a household waste model. Int J Sci Eng Res 5(1):1878–1883
21. U.S. EPA (2014) Method 6020B (SW-846): inductively coupled plasma-mass spectrometry. Revision 2. Washington, DC
22. Venkatesh M, Ravi P, Tewari SP (2013) Isoconversional kinetic analysis of decomposition of nitroimidazoles: Friedman method vs Flynn-Wall-Ozawa method. J Phys Chem A 117:10162–10169. https://doi.org/10.1021/jp407526r
23. Kissinger HE (1957) Reaction kinetics in differential thermal analysis. Anal Chem 29:1702–1706. https://doi.org/10.1021/ac60131a045
24. Ateş F, Büyüktuncer H, Yaşar B et al (2019) Comparison of non-catalytic and catalytic fast pyrolysis of pomegranate and grape marcs under vacuum and inert atmospheres. Fuel 255:115788. https://doi.org/10.1016/j.fuel.2019.115788
25. Ateş F, Miskolczi N, Borsodi N (2013) Comparision of real waste (MSW and MPW) pyrolysis in batch reactor over different catalysts. Part I: product yields, gas and pyrolysis oil properties. Bioresour Technol 133:443–454. https://doi.org/10.1016/j.biortech.2013.01.112
26. Alvarez J, Amutio M, Lopez G et al (2015) Fast co-pyrolysis of sewage sludge and lignocellulosic biomass in a conical spouted bed reactor. Fuel 159:810–818. https://doi.org/10.1016/j.fuel.2015.07.039
27. Loy ACM, Yusup S, How BS et al (2019) Uncertainty estimation approach in catalytic fast pyrolysis of rice husk: thermal degradation, kinetic and thermodynamic parameters study. Bioresour Technol 294:122089. https://doi.org/10.1016/j.biortech.2019.122089
28. Barneto AG, Carmona JA, Alfonso JEM, Blanco JD (2009) Kinetic models based in biomass components for the combustion and pyrolysis of sewage sludge and its compost. J Anal Appl Pyrolysis 86:108–114. https://doi.org/10.1016/j.jaap.2009.04.011
29. Conesa JA, Marcilla A, Prats D, Rodriguez-Pastor M (1997) Kinetic study of the pyrolysis of sewage sludge. Waste Manag Res 15:293–305. https://doi.org/10.1177/0734242X9701500307
30. Djaeni M, Bartels P, Sanders J et al (2007) Multistage zeolite drying for energy-efficient drying. Dry Technol 25:1053–1067. https://doi.org/10.1080/07373930701396535
31. da Silva JCG, Alves JLF, de Araujo Galdino WV et al (2018) Pyrolysis kinetic evaluation by single-step for waste wood from reforestation. Waste Manag 72:265–273. https://doi.org/10.1016/j.wasman.2017.11.034
32. Baroni ÉDG, Tannous K, Rueda-Ordóñez YJ, Tinoco-Navarro LK (2016) The applicability of isoconversional models in estimating the kinetic parameters of biomass pyrolysis. J Therm Anal Calorim 123:909–917. https://doi.org/10.1007/s10973-015-4707-9

33. Abdelouahed L, Leveneur S, Vernieres-Hassimi L et al (2017) Comparative investigation for the determination of kinetic parameters for biomass pyrolysis by thermogravimetric analysis. J Therm Anal Calorim 129:1201–1213. https://doi.org/10.1007/s10973-017-6212-9
34. Scott SA, Dennis JS, Davidson JF, Hayhurst AN (2006) Thermogravimetric measurements of the kinetics of pyrolysis of dried sewage sludge. Fuel 85:1248–1253. https://doi.org/10.1016/j.fuel.2005.11.003
35. Casajus C, Abrego J, Marias F et al (2009) Product distribution and kinetic scheme for the fixed bed thermal decomposition of sewage sludge. Chem Eng J 145:412–419. https://doi.org/10.1016/j.cej.2008.08.033
36. Soria-Verdugo A, Goos E, Morato-Godino A et al (2017) Pyrolysis of biofuels of the future: sewage sludge and microalgae—thermogravimetric analysis and modelling of the pyrolysis under different temperature conditions. Energy Convers Manag 138:261–272. https://doi.org/10.1016/j.enconman.2017.01.059
37. Jindarom C, Meeyoo V, Rirksomboon T, Rangsunvigit P (2007) Thermochemical decomposition of sewage sludge in CO2 and N2 atmosphere. Chemosphere 67:1477–1484. https://doi.org/10.1016/j.chemosphere.2006.12.066
38. Guan Y, Liu C, Peng Q et al (2019) Pyrolysis kinetics behavior of solid leather wastes. Waste Manag 100:122–127. https://doi.org/10.1016/j.wasman.2019.09.005
39. Fong MJB, Loy ACM, Chin BLF et al (2019) Catalytic pyrolysis of Chlorella vulgaris: kinetic and thermodynamic analysis. Bioresour Technol 289:121689. https://doi.org/10.1016/j.biortech.2019.121689
40. Zhang X, Han Y, Li Y, Sun Y (2017) Effect of heating rate on pyrolysis behavior and kinetic characteristics of siderite. Minerals 7:211. https://doi.org/10.3390/min7110211
41. Müsellim E, Tahir MH, Ahmad MS, Ceylan S (2018) Thermokinetic and TG/DSC-FTIR study of pea waste biomass pyrolysis. Appl Therm Eng 137:54–61. https://doi.org/10.1016/j.applthermaleng.2018.03.050
42. Kaur R, Gera P, Jha MK, Bhaskar T (2018) Pyrolysis kinetics and thermodynamic parameters of castor (Ricinus communis) residue using thermogravimetric analysis. Bioresour Technol 250:422–428. https://doi.org/10.1016/j.biortech.2017.11.077
43. Xiang Y, Xiang Y, Wang L (2017) Kinetics of the thermal decomposition of poplar sawdust. Energy Sources Part A Recover Util Environ Eff 39:213–218. https://doi.org/10.1080/15567036.2016.1212291
44. Xie Q, Peng P, Liu S et al (2014) Fast microwave-assisted catalytic pyrolysis of sewage sludge for bio-oil production. Bioresour Technol 172:162–168. https://doi.org/10.1016/j.biortech.2014.09.006
45. Huang Y-F, Shih C-H, Chiueh P-T, Lo S-L (2015) Microwave co-pyrolysis of sewage sludge and rice straw. Energy 87:638–644. https://doi.org/10.1016/j.energy.2015.05.039
46. Wang X, Deng S, Tan H et al (2016) Synergetic effect of sewage sludge and biomass co-pyrolysis: a combined study in thermogravimetric analyzer and a fixed bed reactor. Energy Convers Manag 118:399–405
47. Fan H, Zhou H, Wang J (2014) Pyrolysis of municipal sewage sludges in a slowly heating and gas sweeping fixed-bed reactor. Energy Convers Manag 88:1151–1158. https://doi.org/10.1016/j.enconman.2014.05.043
48. Pokorna E, Postelmans N, Jenicek P et al (2009) Study of bio-oils and solids from flash pyrolysis of sewage sludges. Fuel 88:1344–1350. https://doi.org/10.1016/j.fuel.2009.02.020
49. Sánchez ME, Menéndez JA, Domínguez A et al (2009) Effect of pyrolysis temperature on the composition of the oils obtained from sewage sludge. Biomass Bioenergy 33:933–940. https://doi.org/10.1016/j.biombioe.2009.02.002
50. Akhtar J, Saidina Amin N (2012) A review on operating parameters for optimum liquid oil yield in biomass pyrolysis. Renew Sust Energ Rev 16(7):5101–5109
51. Menéndez JA, Domínguez A, Inguanzo M, Pis JJ (2004) Microwave pyrolysis of sewage sludge: analysis of the gas fraction. J Anal Appl Pyrolysis 71:657–667. https://doi.org/10.1016/j.jaap.2003.09.003
52. Lin J, Sun S, Ma R et al (2018) Characteristics and reaction mechanisms of sludge-derived bio-oil produced through microwave pyrolysis at different temperatures. Energy Convers Manag 160:403–410. https://doi.org/10.1016/j.enconman.2018.01.060
53. Sun Y, Jin B, Wu W et al (2015) Effects of temperature and composite alumina on pyrolysis of sewage sludge. J Environ Sci 30:1–8. https://doi.org/10.1016/j.jes.2014.10.010
54. Zainan NH, Srivatsa SC, Li F, Bhattacharya S (2018) Quality of bio-oil from catalytic pyrolysis of microalgae Chlorella vulgaris. Fuel 223:12–19. https://doi.org/10.1016/j.fuel.2018.02.166
55. Kantarli IC, Yanik J (2009) Use of waste sludge from the tannery industry. Energy Fuels 23:3126–3133. https://doi.org/10.1021/ef8011068
56. Asomaning J, Mussone P, Bressler DC (2014) Thermal cracking of free fatty acids in inert and light hydrocarbon gas atmospheres. Fuel 126:250–255. https://doi.org/10.1016/j.fuel.2014.02.069
57. Rushdi AI, Ritter G, Grimalt JO, Simoneit BRT (2003) Hydrous pyrolysis of cholesterol under various conditions. Org Geochem 34:799–812. https://doi.org/10.1016/S0146-6380(03)00016-0
58. Williams PT, Horne PA (1995) The influence of catalyst type on the composition of upgraded biomass pyrolysis oils. J Anal Appl Pyrolysis 31:39–61. https://doi.org/10.1016/0165-2370(94)00847-T
59. Rezaei PS, Shafaghat H, Daud WMAW (2014) Production of green aromatics and olefins by catalytic cracking of oxygenate compounds derived from biomass pyrolysis: a review. Appl Catal A Gen 469:490–511
60. Miskolczi N, Ateş F (2016) Thermo-catalytic co-pyrolysis of recovered heavy oil and municipal plastic wastes. J Anal Appl Pyrolysis 117:273–281. https://doi.org/10.1016/j.jaap.2015.11.005
61. Wang D, Xiao R, Zhang H, He G (2010) Comparison of catalytic pyrolysis of biomass with MCM-41 and CaO catalysts by using TGA-FTIR analysis. J Anal Appl Pyrolysis 89:171–177. https://doi.org/10.1016/j.jaap.2010.07.008